SAND2016-6456 J

Comparison of the Safety-related Physical and Combustion Properties of Liquid Hydrogen and Liquid Natural Gas in the Context of the SF-BREEZE High-Speed Fuel-Cell Ferry

L.E. Klebanoff,[1,*] J.W. Pratt[1] and C.B. LaFleur[2]

[1]Sandia National Laboratories, Livermore CA 94551

[2]Sandia National Laboratories, Albuquerque, NM 87185

*Author to whom correspondence should be addressed

Abstract:

We review liquid hydrogen (LH_2) as a maritime vessel fuel, from descriptions of its fundamental properties to its practical application and safety aspects, in the context of the San Francisco Bay Renewable Energy Electric Vessel with Zero Emissions (SF-BREEZE) high-speed ferry. Since marine regulations have been formulated to cover liquid natural gas (LNG) as a primary propulsion fuel, we frame our examination of LH_2 as a comparison to LNG, for both maritime use in general, and the SF-BREEZE in particular. Due to weaker attractions between molecules, LH_2 is colder than LNG, and evaporates more easily. We describe the consequences of these physical differences for the size and duration of spills of the two cryogenic fuels. The classical flammability ranges are reviewed, with a focus on how fuel buoyancy modifies these combustion limits. We examine the conditions for direct fuel explosion (detonation) and contrast them with initiation of normal (laminar) combustion. Direct fuel explosion is not a credible accident scenario for the SF-BREEZE. For both fuels, we review experiments and theory elucidating the deflagration to detonation transition (DDT). LH_2 fires shorter duration than energy-equivalent LNG fires, and produce significantly less thermal radiation. The thermal (infrared) radiation from hydrogen fires is also strongly absorbed by humidity in the air. Hydrogen permeability is not a leak issue for practical hydrogen systems. We describe the chemistry of hydrogen and methane at iron surfaces, clarifying their impact on steel-based hydrogen storage and transport materials. These physical, chemical and combustion properties are pulled together in a comparison of how a LH_2 or LNG pool fire on the Top Deck of the SF-BREEZE might influence the structural integrity of the aluminum deck. Neither pool fire scenario leads to net heating of the aluminum decking. Overall, LH_2 and LNG are very similar in their physical and combustion properties, thereby posing similar safety risks. For ships utilizing LH_2 or LNG, precautions are needed to avoid fuel leaks, minimize ignition sources, minimize confined spaces, provide ample ventilation for required confined spaces, and to monitor the enclosed spaces to ensure any fuel accumulation is detected far below the fuel/air mix threshold for any type of combustion.

Introduction:

Keller et al. [1] have provided a compelling argument that if we are going to solve our fuel resource insecurity, political energy insecurity and environmental sustainability problems that accompany our current fossil-fuel-based energy infrastructure, we as a civilization are going to need to turn to hydrogen. For significant environmental benefits, particularly reduction of greenhouse gas (GHG) emissions, the hydrogen will need to be produced by renewable methods with minimal (close to zero) pathway GHG emissions. One can define a zero-carbon energy solution as an energy system in which there is no net release of CO_2 or other GHGs into the atmosphere, either at the point of technical use, or along the path used to produce the fuel. Unless we have a new transportation technology with emissions reductions approaching 80% or more, the emission reductions will not be robust against growth in either population, or growth in the intensity with which technology uses energy [1]. While use of fossil-based hydrogen allows the introduction of the hydrogen-based power conversion technology [2], ultimately, renewable hydrogen is required. The time-scales for technological change and the ~ 50-year horizon associated with our limited fossil fuel resources indicate that we have to start the conversion to a renewable hydrogen technology now, and we need to be going much faster than we are [1].

As reviewed by Klebanoff et al. [2], high efficiency hydrogen energy conversion devices that convert hydrogen into electrical or shaft power are powerful drivers for hydrogen technology. These conversion devices include hydrogen internal combustion engines (ICEs), both spark ignition and turbine hydrogen engines, along with hydrogen fuel cells [2]. Proton Exchange Membrane (PEM) fuel cells in particular are already finding use in the first fuel cell vehicles, portable power, backup power, material handling equipment and fuel cell mobile lighting [2]. The use of hydrogen fuel cell technology for maritime applications is currently being considered.

The San Francisco Bay Area Renewable Energy Electric Vessel with Zero Emissions (SF-BREEZE) is a conceptual high-speed hydrogen fuel cell ferry designed for commercial use in the San Francisco Bay. The SF-BREEZE combines renewable liquid hydrogen (LH_2), PEM fuel cell technology, and a catamaran hull design to provide high-speed ferry service for 150 passengers at 35-knot top speed. The feasibility of such a vessel has been proven in a project funded by the Maritime Administration (MARAD) within the U.S. Department of Transportation. The technical and economic feasibility of the vessel, its initial design, as well as the extent to which new maritime regulations will be required to permit safe use of hydrogen fuel cell technology in the ferry application will be reported elsewhere [3].

During the project, we analyzed the use of LH_2 onboard the SF-BREEZE with a focus on safety. Another cryogenic fuel, liquid natural gas (LNG), has been finding increasing use as a primary propulsion fuel for maritime vessels. Since maritime regulations have been formulated to cover LNG use as a primary propulsion fuel, it was natural that our examination of the safe use of LH_2 as a primary fuel for ferries be couched as a comparison to LNG, for both the maritime

environment generally, and specifically for the SF-BREEZE. This comparison required pulling information from many sources in order to form a complete picture of the differences between LH_2 and LNG as practical maritime fuels. Here we review both the physical and chemical nature of these fuels that impact safety, as well as the very different character of the fires derived from burning LH_2 and LNG. We supplement this existing information with new analyses that shed additional light on the uses of LH_2 and LNG in marine applications.

It is timely to compare and contrast the physical and combustion properties of LH_2 and LNG. In 1978, Hord provided [4] an excellent and comprehensive comparison of the safety properties of hydrogen and methane (the primary constituent of NG), with both fuels being compared to gasoline. In 1981, Donakowski [5] assessed LH_2 and LNG physical and combustion properties with regard to safety. Also in the early 1980's NASA sponsored separate work by Lockheed and the Arthur D. Little Company to investigate hydrogen-fueled commercial aircraft. Both studies involved technical and safety comparisons between LH_2, LNG and conventional jet fuel (Jet-A) in their use as primary aviation fuels. Brewer has published the results of the Lockheed work in both journal [6] and book [7] form. The results of the A.D. Little study were summarized in several NASA reports in 1960, 1964 and 1982 [8 - 10]. The comparative properties of LH_2 and LCH_4 for aviation were later reviewed by Contreras and co-workers in 1997 [11], who also reviewed some subsequent designs for LH_2 aircraft conceived by the Airbus consortium and Boeing. In many ways, hydrogen use in aircraft is similar to its use in high-speed ferries, as both aircraft and high-speed watercraft are very weight-sensitive applications, favoring storing hydrogen on-board as a liquid. Safety comparisons between compressed natural gas and compressed hydrogen as automotive fuels were reported by Karim in 1983 [12].

Since these prior comparisons, there has been significant progress in elucidating the combustion properties of hydrogen, particularly with regard to the effects of buoyancy and turbulent mixing on combustion and the "deflagration to detonation transition" (DDT). Advanced modeling studies have also clarified how cryogenic fuels spread and vaporize when spilled on the ground or other surfaces. In addition, there have been a couple of decades of further experience handling LH_2 and LNG, and development of associated codes and standards. Here we provide an updated review with these new developments, with a focus appropriate for the comparison of LH_2 and LNG in maritime applications generally, and for the specific case of the SF-BREEZE.

Design of the SF-BREEZE as a Model of Hydrogen Use in Maritime Applications:

Figure 1 displays engineering models of the SF-BREEZE [3]:

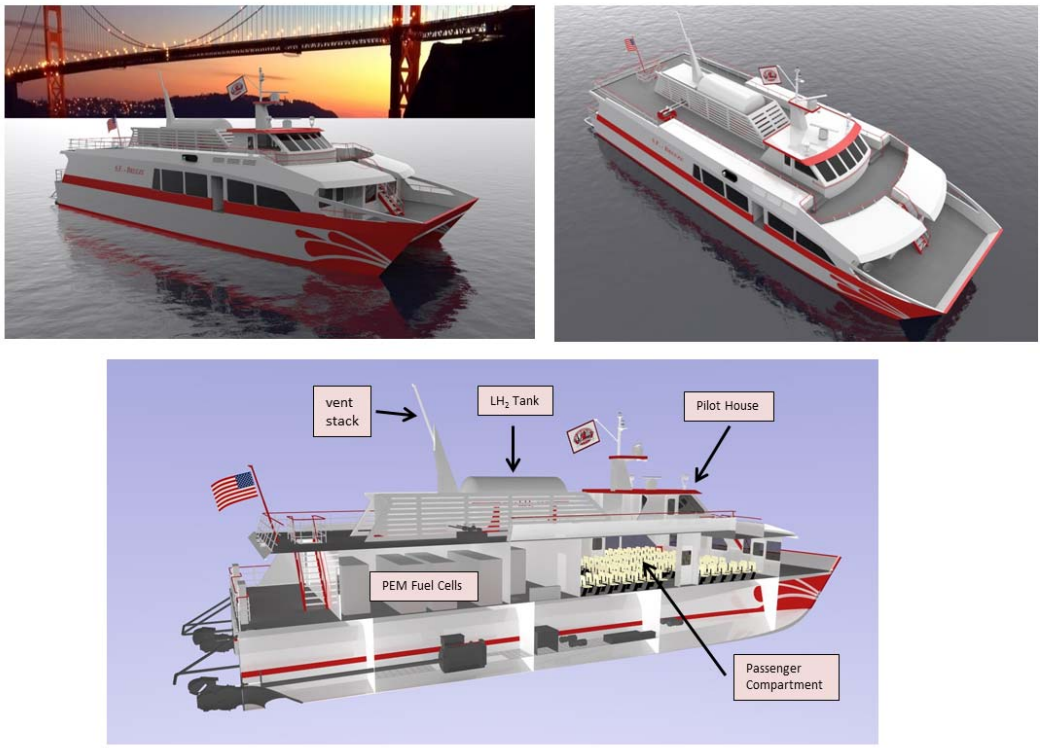

Figure 1: Engineering Models of the SF-BREEZE. The Top Deck holds the LH_2 storage tank, the associated vent stack, evaporation equipment, and the Pilot House of the vessel. The Main Deck holds the PEM fuel cell power racks and the passenger compartment.

The Top Deck holds a cylindrical 1200 kg capacity LH_2 tank, with enough hydrogen for 4 hours of continuous operation. A desire to refuel only a couple of times per day drives the 1200 kg capacity specification. The high-speed (35 knots) requirements of the design requires the lightest method of storing 1200 kg of hydrogen, namely LH_2 storage in a DOT-approved double walled cryogenic tank. The fuel cell racks are located on the Main Deck, adjacent to the passenger compartment. The fuel cells are of the PEM variety, selected for their fast turn on, minimal weight, commercial availability, established track record and ability to run on pure hydrogen. Although PEM fuel cells can use "industrial grade" hydrogen (99.95% pure), LH_2 is typically 99.9995% pure.

Unlike hydrogen derived from LH_2, LNG is a mixture with composition that varies depending on place of origin. LNG is typically ~ 93% methane, ~ 5% ethane, with the balance being propane, butane, nitrogen and other trace gases. The percentage of methane runs from 87% to 96% depending on source [13]. While in some cases the approximation is made that the physical and combustion properties of LNG can be fairly represented by those of liquid methane (LCH_4), it is

worth noting that the composition variations do have observable effects (typically modest) on the combustion properties [14] and the net GHG emissions associated with LNG combustion [13]. The fact that LNG consists of a mixture introduces the phenomenon of compositional "stratification" whereby density and temperature differences arising from the mixture can lead to increased local vaporization (called rollover) [15].

Physical Properties of Hydrogen and Methane:

Gaseous State:

Hydrogen is the lightest gas, with a density of 0.08376 kg/m^3 at normal temperature and pressure (NTP), 293.15K, 1 atmosphere pressure. Methane is considerably heavier, with a density at NTP of 0.65119 kg/m^3. Both gases at NTP are more buoyant than air, which has a NTP density of 1.204 kg/m^3. It is generally not possible to accurately specify the "rising velocity" of a practical hydrogen or methane release, because the terminal rising velocity is established as a balance of the buoyant force (pointed up), gravitational force (pointed down), and the atmospheric drag (pointed down) on the gas volume as it rises. The atmospheric drag depends on the shape and cross-sectional area of the released gas volume, which in practical releases is unknown and can depend on the initial conditions of the release, turbulence and wind conditions. Furthermore, the density of air depends on relative humidity. To give a sense of the relative rising rates for hydrogen and methane at NTP for spherical volumes of released gas in the absence of wind or turbulence, we show in Figure 2 a plot of the terminal rising velocity in air (under these assumptions) for both gases. For the hydrogen fuel complement of the SF-BREEZE (1200 kg), this mass of hydrogen would, at NTP, occupy a sphere with radius 15.07 m, with a terminal rising velocity of 27.92 m/s. The same mass of methane would occupy a sphere of radius 7.61 m with terminal rising velocity of 13.93 m/s. Clearly, hydrogen is significantly more buoyant than methane, although both rise quickly in air at NTP.

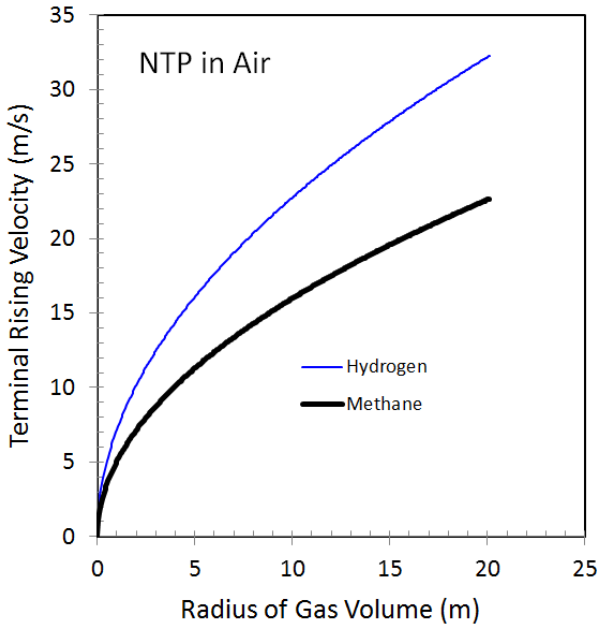

Figure 2: The terminal rising velocity for spherical volumes of hydrogen and methane in air at NTP (293.15 K, 1 atmosphere pressure). The figure uses NTP gas densities of 1.204 kg/m^3 for air, 0.08376 kg/m^3 for hydrogen and 0.65119 kg/m^3 for methane.

Being a homolytic diatomic molecule, hydrogen has no dipole moment, and vibrations of the molecule cannot produce charge separation along the bond axis. Consequently, hydrogen does not interact with infrared radiation, and is not a greenhouse gas. In contrast, since methane is a heterolytic molecule with different elements bonded together, the bonds are inherently polar, and stretches and bends of C-H bonds produce charge fluctuations that can couple to infrared electromagnetic radiation. This character makes methane a potent greenhouse gas, ~ 23 times more capable of trapping heat in the atmosphere than CO_2. This fundamental difference between hydrogen and methane makes methane leaks from LNG infrastructure a serious environmental concern and an economic loss, whereas leaks from a hydrogen infrastructure would have only an economic impact.

Liquid State:

A defining characteristic of molecular hydrogen is the very weak attractive van der Waals interactions between H_2 molecules. The intermolecular attractions between H_2 molecules are weaker than those between CH_4 molecules, which explains the lower boiling temperature for LH_2 compared to LCH_4 (LNG). The normal boiling point for hydrogen is 20 K; the normal boiling point for LCH_4 is 111 K. An important consequence for the difference in boiling points is that liquid methane (at its boiling point) cannot liquefy air, whereas LH_2 can liquefy air, whose components N_2 and O_2 condense at 77.3 K and 90.2 K, respectively. These atmospheric gases can also solidify when exposed to LH_2, as the melting points for solid N_2 and solid O_2 are 63.3 K and 54.8 K, respectively. The potential for liquefying or solidifying air introduces safety

concerns arising from clogging hydrogen lines with condensed air, as well as concerns about reactivity stemming from condensed oxygen. As a practical matter, these air condensation issues are routinely handled in LH_2 fueling operations by purging the LH_2 plumbing lines with hydrogen or helium (more typically hydrogen due to its availability at the site and lower cost).

The weak intermolecular attraction between H_2 molecules, combined with hydrogen's low mass, makes LH_2 a low-density fluid. The density of LH_2 is 71 g/L at its normal boiling point (NBP) of 20 K at 1 atmosphere pressure. The density of LCH_4 at its NBP of 111 K at 1 atmosphere pressure is 422 g/L. For comparison, the density of liquid water is 1000 g/L. For the same amount of stored energy, LH_2 has 0.38 times the mass of LCH_4, but has 2.4 times the volume.

Both hydrogen and methane are less dense than air at room temperature and pressure. An important safety-related question is: when these liquids evaporate, producing either cold hydrogen gas at 20 K, or cold methane gas at 111 K, how much do these gases have to warm before they become more buoyant than ambient air? If we assume that for small leaks, the ambient air is not cooled too much and remains near NTP, then hydrogen will become more buoyant than NTP air (with density 1.204 kg/m^3) at 22.07 K [16]. In other words, hydrogen release from LH_2 need only warm up by ~ 2 K in order to become more buoyant than air at NTP conditions. In contrast, methane needs to warm up 53.3 K, from 111 K to 164.3 K, before its gas-phase density equals that of NTP air [16]. As a result, when LCH_4 evaporates at 111 K, the cold methane gas stays non-buoyant for significantly longer times than does LH_2. Both LH_2 and LNG at their NPB expand considerably when warmed to NTP. The volume expansion factor for hydrogen is 847.6 and that for methane is 648.0 when a given mass is warmed from the NPB to NTP.

Cryogenic Spills:

The weak intermolecular attractions between hydrogen molecules leads to the enthalpy of vaporization ΔH_{vap} of LH_2 being only 0.92 kJ/mole, 9.2 times less than that of LCH_4, whose ΔH_{vap} value is 8.5 kJ/mole [17]. For comparison, the ΔH_{vap} of liquid water is 40.66 kJ/mole, due to the strong hydrogen bonding found between water molecules. The extraordinarily low ΔH_{vap} value for hydrogen has important consequences for its use as a fuel and its behavior during spills. For equal amounts of stored energy (to be discussed), LH_2 takes 3 times less thermal energy to evaporate than LCH_4. Thus, in a spill, LH_2 will cool surrounding surfaces much less than a LCH_4 (LNG) spill. This is an important consideration for structural elements of a ferry, as mild ferritic steels can undergo brittle fracture when exposed to cryogenic temperatures [18]. The Top Deck of the SF-BREEZE is made of aluminum, which does not suffer brittle fracture [19].

We have analyzed the effect of spilling the entire 1200 kg LH_2 fuel complement onto the Top Deck of the SF-BREEZE, although we note that since the cryogenic tanks designed for LH_2 have no history of catastrophically failing in this way, the U.S. Coast Guard does not consider such a spill a credible accident scenario. In such a spill, the SF-BREEZE Top Deck, with area 162.65

m^2, thickness 0.794 cm and mass 3483 kg would be cooled from 298 K to 168 K. The cooling of the aluminum deck is deeper if LCH_4 is spilled, due to the significantly higher ΔH_{vap} value of 8.5 kJ/mole. For the same Top Deck, spilling an energy-equivalent mass of LCH_4 (3198 kg) cools the Top Deck from 298 K to 111 K. Thus, due to the higher ΔH_{vap} value for methane, spills of LCH_4 will produce deeper reductions in temperature of structural items than spills of LH_2. The chemistry and physics of how LH_2 and LNG behave when spilled are important for understanding not only thermal effects on the surroundings, but also the behavior of such pools if their vapors are ignited (so called "pool fires.") We will return to this topic later when we discuss the nature of pool fires in the maritime application.

The A.D. Little Company [10] performed an early comparison of LH_2 and LNG (LCH_4) in the context of cryogenically fueled commercial aircraft. This work concentrated on the combined problem of fluid flow when in contact with the ground along with ignition. Witcofski and Chirivella at NASA Langley [20] conducted the first large-scale spill tests of LH_2 in the absence of ignition, with a focus on the measured hydrogen content of vapor clouds at varying distances from the pool spill. This NASA work motivated subsequent work on predicting the duration and physical extent of LH_2 spills, as well as those of other cryogens including LCH_4. Verfonden and Dienhart performed pioneering model studies of the NASA experiments and conducted controlled spill tests focusing on the extent and duration of LH_2 spilled onto water and aluminum [21, 22], two surfaces very relevant for the SF-BREEZE application. These workers also developed a mathematical model called LAuV to address the relevant phenomena involved in cryogenic pool spreading and vaporization. The LAuV model predictions for pool radius and duration received prior validation by comparison with LNG pool spreading experiments.

The NASA spill tests did not emphasize the size and duration of the LH_2 pool, but one spill trial did provide data that a spill of 5.7 m^3 (404.7 kg) of LH_2 produced a maximal radius of 2 - 3 meters and the entire pool evaporated within 5 seconds after cessation of active spilling (with occurred after 38 seconds). Verfonden and Dienhart's model of this spill test predicted a LH_2 radius of 6.5 m, and excellent agreement with the duration data [21, 22]. These foundational studies point to LH_2 spills having very short durations and relatively small physical extents, both attributable to the high vaporization rate produced by the low ΔH_{vap} value. Heat conduction from the ground is the dominant contributor to evaporation of spilled pools of cryogenic liquids [21, 22].

The LAuV model gave an excellent account of the controlled LH_2 spill tests on both water and aluminum [21, 22]. Experimentally, the duration of the pool was determined mostly by the practical speed at which LH_2 could be physically spilled, which was 62 seconds in these tests. For example, for 0.31 m^3 (22.0 kg) of LH_2 spilled on water, the observed and calculated pool radii were both ~ 0.6 m, and the model predicted the pool completely evaporated at 62.9 seconds, within 1 second of completion of fuel spill. Spills onto water had a larger radius (0.6 m vs. 0.4 m) than those on aluminum due to ice formation and the subsequent poorer heat transfer to the LH_2 pool. Overall, spill results on water or solid surfaces were comparable in size and duration.

The LAuV model was also used to predict the pool radii and vaporization times (duration) for 40 m^3 instantaneous spills of the LH_2 and LNG (modeled as 87% methane and 13% propane) on solid ground. Table I summarizes these results [21].

Table I: Predicted Size and Duration of Instantaneous LH_2 and LNG Spills from LAuV Model, from Reference [21].

Pool Characteristic	LH_2 (17,040 kg)	LH_2 (2,840 kg)	LNG (40,725 kg)*	LNG (18,000 kg)*
Radius (m)	42	20	49	38
Duration (s)	25	13	80	65

*assumes an LNG density of 450 g/L

It is clear from Table I that due to the exceptionally low ΔH_{vap} value, LH_2 spills are very short duration events. We estimate for the SF-BREEZE that if the entire 1200 kg contents of the LH_2 tank instantaneously spilled onto the Top Deck, the cryogenic pool would last ~ 6 seconds and spread to a maximal radius of ~ 8 meters.

More recently, theory was extended to account not only for the dimensions of the LH_2 pool, but also for the composition of the vapor phase immediately above the pool. Middha and co-workers [23] used a 3-D computational fluid dynamics (CFD) code named FLACS to simulate the NASA and the Verfonden and Dienhart experiments for both pool formation and hydrogen content in the air above the pool and downrange. The FLACS and LAuV models were in general agreement with each other with regard to pool formation (radius, duration), although the FLACS model had higher evaporation rates and smaller pool radii due to the inclusion of thermal effects other than ground conduction. The FLACS model gave a reasonable account (with factors of 2) of the gas dispersion data that was available. The FLACS model did not take into account possible gas-phase complications such as the condensation of air components (oxygen, nitrogen) in the hydrogen cloud or perhaps N_2 and O_2 freezing very close to the LH_2 pool, or in the pool itself. Condensation or freezing of atmospheric water was not included the FLACS model studies [23]. The condensation/freezing of atmospheric components (water, O_2, N_2) is at the edge of the state-of-the-art in theoretical modeling of spilled cryogenic pools.

Two other physical phenomena need to be described for hydrogen use in maritime applications: hydrogen permeation and hydrogen embrittlement.

Permeation:

Hydrogen permeation arises from the dissociation of molecular hydrogen at metal and oxide surfaces into hydrogen atoms, and the subsequent diffusion of hydrogen atoms through materials involved in hydrogen storage and plumbing lines. Hydrogen atoms produced in this way can also lead to hydrogen embrittlement, which is a very important phenomenon in materials science. Many misinterpret hydrogen permeation (even in the absence of embrittlement) as a leak risk.

The concern is that hydrogen diffusing through tubing and other fittings can pass though the material and exit as hydrogen gas, thereby constituting a leak.

Permeation as a source of leaking is not an issue for the practical performance of tubing, valves or other hardware because the quantities of gas exiting in this way are infinitesimal. San Marchi, and co-workers have described hydrogen permeation in stainless steels at high pressure [24], reviewing the fundamental thermodynamics and kinetics of hydrogen permeation, diffusion and solubility in a material supporting a hydrogen pressure differential. Hydrogen permeation is defined as the product $D \cdot K$, where D is the diffusivity and K is the equilibrium constant for hydrogen dissolving from the gas phase into a material. We now assess hydrogen dissolution, permeation and diffusion in metals as a leak risk using experimentally determined values for solubility and diffusion in steel alloys [24].

We ask the question: "If the entire 1200 kg fuel complement of the SF-BREEZE LH_2 tank were vaporized to room temperature, and compressed to 150 psi (the maximal pressure to be found anywhere on the SF-BREEZE), what would the rate of hydrogen diffusion be through 1/16" thick 300 series (304, 316) stainless steel?" This corresponds to the maximal hydrogen permeation conditions (highest temperature, highest pressure, smallest hardware wall thickness) that could exist in the SF-BREEZE hydrogen-fueling manifold. Studies show the solubility, permeation and diffusion of hydrogen in 304 and 316 alloys are the same to within experimental accuracy [24]. If one takes the entire 1200 kg of hydrogen, vaporizes it to room temperature, and enclosed it in a spherical 316 container and compressed the gas to 150 psi, the sphere would have a radius of 7.0 m. Assuming a 1/16" wall thickness for the sphere, we can calculate the rate of passage of hydrogen from the interior of the sphere to the exterior, exiting the sphere as hydrogen gas "leaking" across its entire external surface area. Under these circumstances, the flux of hydrogen out of the sphere in steady state would be 1.56×10^{-9} moles/s. Hydrogen diffusion is a thermally activated process, and drops off drastically as the temperature is lowered. At 200 K, the rate of flux would be 1.13×10^{-14} moles/s, which shows how dramatically this thermally activated process is reduced for even mildly cryogenic conditions.

This leakage rate of 1.56×10^{-9} moles/s needs context. If one were to fill a classic model KS-21716 AT+T telephone booth (dimensions H x W x D = 211 cm x 85 cm x 85 cm) with this permeation leakage of hydrogen, it would take 60 years to reach the 4% LFL. One might ask how much hydrogen the 150 passengers on the SF-BREEZE are releasing. Hydrogen is a well-known product of human metabolism, produced at ~ 3 ppm levels in human respiration. Assuming an average human lung tidal volume of 0.5 liters/breath, and a respiration rate of 20 breaths /minute, one can readily calculate that it would take 10.3 days for the hydrogen from passenger respiration, directed into the KS-21716 phone booth, to reach the 4% LFL. This assumes of course that only hydrogen from the respiration enters the phone booth. The point of this discussion is that permeation in the context of the SF-BREEZE is not an issue for leakage from plumbing systems such as valves, fittings, tubes, pipes, etc. because it is infinitesimal. Passenger breathing represents a vastly larger source of hydrogen. It is also worth noting that

welds do not strongly affect the rate of diffusion in metal samples, and there is some evidence microscopic defects in welds can actually act as hydrogen traps, slowing diffusion.

One might reasonably ask if CH_4 containment can lead to molecular dissociation, releasing hydrogen atoms into a vessel wall material where they can then diffuse, resulting in permeation and perhaps even hydrogen embrittlement. The surface science of methane adsorbed on iron is very different from hydrogen adsorbed on iron. In investigations both experimental [25] and theoretical [26], methane bonds to iron films in a very weakly bound "physisorbed" state, characterized by thermal desorption from the surface at 130 K. Methane does not adsorb to iron surfaces at room temperature. Even for temperatures below 130 K in which methane is bound to iron, there is no dissociation into hydrogen and carbon, because the energy barrier for breaking the C-H bonds is unfavorable [27]. In contrast, hydrogen is dissociated at iron surfaces as revealed in theoretical [27] and experimental [28] studies, forming bound chemisorbed H atoms that are stable at room temperature and desorb only if the temperature is raised to greater than ~ 625 K. This basic surface science explains why methane does not dissociate at stainless steel surfaces (with majority component iron), and as a result is not a source of hydrogen atom production at internal natural gas plumbing or storage surfaces that would lead to hydrogen permeation or hydrogen embrittlement.

Hydrogen Embrittlement:

Hydrogen solution, permeation and diffusion, even though involving vanishingly small quantities of hydrogen from a leak perspective, are key ingredients to the phenomenon of hydrogen embrittlement. Hydrogen embrittlement is a significant area of materials science, and it is beyond the scope of this review to cover it in a comprehensive manner. Excellent reviews exist [29]. As described above, hydrogen embrittlement does not exist for materials carrying LNG, NG or methane because there is no methane dissociation at the metallic surface. On the other hand, hydrogen atoms produced by the dissociation of H_2 at metallic surfaces can diffuse into the bulk of the material, and accumulate at defect sites in the presence of material strain (which all practical materials have to some extent). Because of the combination of hydrogen, pre-existing defects and strain, hydrogen atoms can accumulate at defect sites, and form brittle metal hydrides such as FeH_2 and CoH_2. If the pre-existing defect is a small crack, the hydriding of the surrounding metal can lead to facile crack growth and eventual material failure. This is a problem for ferritic (bcc) steels, but not for austenitic (fcc) steels, or copper or aluminum.

As a practical matter, hydrogen embrittlement is circumvented in hydrogen technology by using 304 or 316 stainless steels, aluminum or copper in hydrogen storage systems and piping. Decades of industrial experience show these materials are robust to hydrogen embrittlement. This materials choice is similar in spirit to choosing copper over iron in the manufacture of electrical wiring. Copper has a higher electrical and thermal conductivity than Fe, and using copper reduces resistive losses and promotes thermal control. Similarly, the correct materials must be chosen for hydrogen service. The experience of the gas providers is that hydrogen

embrittlement is not a maintenance issue for LH_2 or other hydrogen infrastructure when these materials choices are properly implemented [30]. Like most commercial LH_2 tanks, the interior liner of the LH_2 tank of the SF-BREEZE will be 304 stainless steel. One could contemplate using lighter weight aluminum for the inner liner, but it is structurally weaker and requires using thicker liners (which mostly defeats the lighter weight advantage), and has an undesirable larger thermal conductivity which increases heat leak.

Combustion Properties of Hydrogen and Methane:

The physical properties just discussed for hydrogen and methane are the foundation for the discussion of the combustion properties of these two fuels. Table II provides values for "classic" physical and combustion properties of hydrogen and methane. The combustion properties are taken in part from Reference 31.

Table II: Physical and Combustion Property Values for Hydrogen and Methane.

Quantity	Hydrogen	Methane
Molecular Weight	2.016	16.043
Density of Gas at NTP, kg/m^3	0.08376	0.65119
Temperature to Achieve NTP Neutral Buoyancy in Air (1.204 kg/m^3), K	22.07	164.3
Normal Boiling Point (NBP), K	20	111
Liquid Density at NBP, g/L	71	422
Enthalpy of Vaporization at NBP, kJ/mole	0.92	8.5
Lower Heating Value, MJ/kg	119.96	50.02
Limits of Flammability in Air, vol%	4 – 75	5.3 - 15
Explosive Limits in Air, vol%	18.3 – 59.0	6.3 – 13.5
Minimum Spontaneous Ignition Pressure, bar	~ 41	~ 100
Stoichiometric Composition in Air, vol%	29.53	9.48
Minimum Ignition Energy, J	0.02	0.29
Flame Temperature in Air, K	2318	2148
Autoignition Temperature, K	858	813
Burning Velocity in NTP Air, m/s	2.6 – 3.2	0.37 – 0.45
Diffusivity in Air, cm^2/s	0.63	0.2

Before discussing the combustion of these fuels by explicit ignition sources, we consider the phenomenon where releases of these gases can spontaneously ignite even in the absence of specific ignition sources.

Spontaneous Ignition:

Dryer and coworkers [32] were among the first to recognize that compressed hydrogen and methane, when suddenly released, can undergo "spontaneous ignition," also called "autoignition." Spontaneous ignition is a particular safety concern, because it represents an ignition pathway that can persist even if one has successfully removed all explicit ignition sources from the design of a particular application involving these fuels. A number of different mechanisms have been considered [33]. The evolving picture is that spontaneous ignition arises when a sufficiently high pressure boundary between the compressed gaseous fuel and surrounding (lower pressure) air results in a shock wave that can rapidly mix and heat fuel and oxygen, leading to ignition and flame propagation fed by the continuing fuel release. Dryer and co-workers [32], along with other investigators [34], have examined spontaneous ignition as a function of release pressure, and downstream hardware configuration, which can affect the course of the shock propagation and reactant mixing. The results show that the tendency to autoignite is higher for hydrogen than methane. The minimum pressure for which spontaneous ignition has been observed, independent of downstream hardware geometry, is ~ 41 bar for hydrogen and ~ 100 bar for methane.

While spontaneous ignition is a concern for hydrogen fuel-cell light-duty vehicles, which currently employ high-pressure (350 bar, 700 bar) hydrogen, the SF-BREEZE employs LH_2 storage of hydrogen. The highest pressure in the SF-BREEZE fueling system will be ~ 10 bar, which corresponds to the pressure relief for the LH_2 tank vent. The manifold inlet pressure to the PEM fuel cells will be ~7 bar. As a result, the overall SF-BREEZE system pressures are too low for spontaneous hydrogen ignition to come into play. The mechanistic cause of spontaneous ignition continues to be an active research topic.

Explicit Ignition:

In order to discuss combustion caused by specific ignition sources, some definitions are in order:

Weak (Thermal) Ignition Sources: Matches, sparks, hot surfaces, open flames with initiation energy of < 50 mJ are called "weak" or "thermal" ignition sources. These are the ignition sources of accidents.

Strong (Shock Wave) Ignition Sources: blasting caps, TNT, high-voltage capacitor shorts (exploding wires), lightning are all examples of "strong" ignition sources with initiation energy of > 4 MJ. Note that strong ignition sources are ~ 10^8 times stronger than weak initiators. This is an enormous difference in ignition input energy. Other than lightning, strong ignition sources are the sources of intentional ignition, not accidental ignition.

Fire: Fire is the term for ordinary combustion familiar in everyday life where the flame propagates through the unburned fuel/air mix at low speeds (~ 20 m/s or less). Fires are not loud, and produce negligible overpressure in the surrounding air. Fires are produced by weak

ignition sources in contact with flammable mixtures of fuel and air. Despite their familiarity, it is important from a safety perspective to remember that fires are dangerous, especially on an isolated vessel.

Deflagration: Fast combustion where the flame propagates through the unburned fuel/air mix rapidly, but at subsonic speeds (~ 100 - 400 m/s). Deflagrations can be loud, and can produce overpressures that can rupture eardrums and cause other injury. Under the right conditions, deflagrations are initiated by weak ignition sources. From a safety perspective, deflagrations are very dangerous.

Explosion or Detonation: The terms explosion and detonation are often used interchangeably, and will be so used here. Explosions are extremely fast combustion events where the flame propagates through the unburned fuel/air mix at supersonic speeds (> 700 m/s). Explosions produce loud bangs and very damaging overpressures. Direct explosions are caused by strong ignition sources with specific conditions of fuel/air mix and confinement. From a safety perspective, explosions and detonations are very, very dangerous.

Fires:

Both H_2 and CH_4 mixtures with air ignite easily using weak ignition sources to produce fires. Fire regulations focus on the "Lower Flammability Limit" (LFL), expressed as a volume percentage (vol%):

$$\text{vol\%} = [\text{Volume (Fuel)}/\text{Volume (Fuel + Air)}] \times 100$$

The LFL is the focus of safety regulations, since the risk of fire typically comes from the accumulation of flammable gas in initially clean air. The classic values [31] for the flammability range (LFL to upper flammability limit (UFL)) for H_2 = 4.0 – 75.0 % at 298 K. The LFL to UFL of methane is = 5.3 – 15.0 % at room temperature [31]. For context, the LFL – UFL values for gasoline are 1 – 7.6% [31]. Thus, while hydrogen has a much wider flammability range than methane (making it more of a fire risk), from the perspective of building up flammable gas in an initially clean environment, hydrogen and methane have similar LFLs, with similar threshold gas accumulations that can be ignited. The minimum ignition energy for H_2 is 0.020 mJ; that for CH_4 is 0.29 mJ. Static discharges from human beings are ~ 10 mJ, so both CH_4 and H_2, when present between the LFL – UFL limits, ignite easily when exposed to with common (weak) ignition sources. Table II lists these combustion properties for hydrogen and methane.

As described by Cashdollar and co-workers [35], in quiescent mixtures of fuel and air, fuel buoyancy alters the LFL required for self-sustaining fires. In a self-sustaining fire, combustion advances at nearly the same speed for upward, horizontal and downward directions. Upward flame propagation is intrinsically faster than other propagation directions because combustion products are hotter and less dense than the original fuel and air mixture. However, for sufficient concentrations of fuel, the combustion is hot enough that flame propagation is facile in all

directions. Hydrogen mixtures ignited at 4 % produce very little heat, and flame propagation is almost exclusively upward. Thus, for a spherical hydrogen/air mixture, weak initiation at the sphere center at the LFL will only produce combustion for a relatively small upper slice of the spherical volume, producing fire that cannot sustain itself to the point of complete combustion of the fuel. For sustained hydrogen fires, the hydrogen/air mix needs to be ~ 8% for combustion to propagate in all three directions with complete combustion of the fuel [35]. Since methane is less buoyant than hydrogen, buoyancy effects are correspondingly less, and full-three dimensional flame propagation is achieved at a methane/air mix of ~ 6%, up from the classic LFL value of 5.3 %.

Interestingly, intentional mixing of the fuel/air mixture can largely counteract the effects of buoyancy. In some of the experiments of Cashdollar et al. [35], a mixing fan produced flows of order 1 – 1.5 m/s along the fan rotation axis. In this mildly turbulent condition, the threshold for a self-sustaining fire in hydrogen returned to 4%. The effect of the active mixing is to introduce a velocity element that can overcome the influence of buoyancy and promote mixing, which produces hotter burning, and faster flame speeds that propagate well in all three directions. For methane, for which buoyancy effects are small to begin with, mild turbulent mixing produced the same ignition concentration threshold as quiescent conditions (5.3%).

In typical accidental scenarios involving slow releases of hydrogen in the SF-BREEZE fuel cell rooms, we anticipate the conditions will correspond more closely to the quiescent scenario, suggesting a LFL for sustained hydrogen combustion to be closer to ~ 8%. Even with ventilation producing the 30 room air exchanges required by U.S. Coast Guard regulations, the average air speed during ventilation would only be ~ 0.02 m/s, which is unlikely to produce strong turbulent flow.

Laboratory experiments have shown that the LFL holds even if the ignition source is highly intermittent. Schefer and coworkers [36] have shown that in ignition tests on hydrogen and methane turbulent jets using a 100-mJ laser with a 9-ns pulsewidth, ignition is not possible unless the instantaneous concentration of fuel present at the time of the laser pulse is above the classic LFL.

Overall, from the point of view of fire risk coming from fuel release into initially clean air, hydrogen and methane have very similar ignition risks because their LFLs are similar.

Explosion and Detonation:

Hydrogen and methane can both detonate given the right conditions of fuel/air mixture, confinement and strength of ignition source. Ng and Lee [37] have discussed the explosion risk for hydrogen in the transportation setting. The lower explosion limit (LEL) of H_2 at room temperature (% by volume) - upper explosion limit (UEL) = 18.3 – 59.0 % at room temperature [31]. The LEL to UEL of methane is = 6.3 – 13.5 % at room temperature [31]. Thus, hydrogen has a much wider explosive range than methane, making it more of an explosion risk in general.

From the perspective of building up flammable gas in an initially clean environment, the LEL of methane (6.3%) is reached considerably sooner than that of hydrogen (18.3%).

In the SF-BREEZE design, hydrogen release is a concern for two locations. On the Top Deck where the LH_2 tank is situated, we have an essentially unconfined environment in which a release of H_2 would be free to disperse upward without blockage. In contrast, the Main Deck holds the PEM fuel cells, which are distributed into a Starboard (right, facing forward) and Port (left, facing forward) Fuel Cell Rooms. A cutaway view of the Main Deck of the SF-BREEZE is shown in Figure 3:

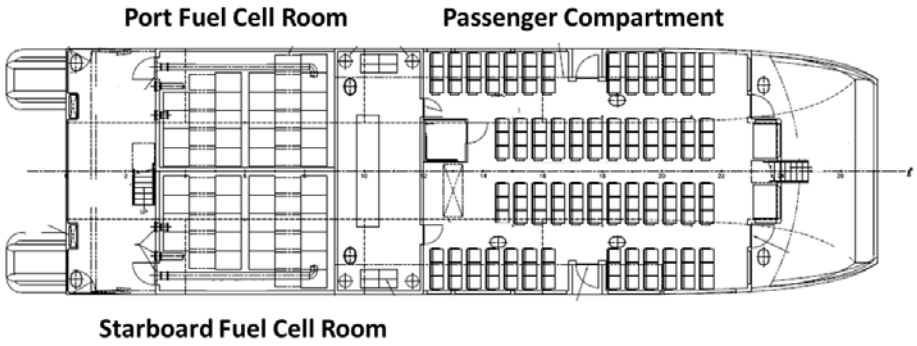

Figure 3: Cutaway view of the Main Deck of the SF-BREEZE. The PEM fuel cells are distributed into a Starboard Fuel Cell Room and a Port Fuel Cell Room, with ~ 20 fuel cell racks in each room. The Passenger Compartment holds 150 passengers. The "beam" (width) of the SF-BREEZE is 10 m. The dimensions of each Fuel Cell Room are 7.4 m long x 5.1 m wide x 2.7 m tall.

In these fuel cell rooms, there exists a confined situation where hydrogen (if released) would enter an enclosed room, albeit with installed ventilation providing 30 room exchanges of air per hour. We examine combustion beyond normal fires to include assessment of explosions and deflagrations with varying degrees of confinement.

The A.D. Little Company evaluated the practical explosion risk from large-scale releases of hydrogen in confined and unconfined environments in a series of experiments and modeling studies for the U.S. Air Force and the NASA Lewis Research Center over the period 1960 – 1982 [8 - 10]. These impressive and comprehensive tests represent the first modern scientific investigations of the consequences of spilling and igniting large quantities of LH_2. The original work, published in 1960 [8] with aspects reported again in 1964 [9], reported the combustion of stoichiometric mixtures of hydrogen and air confined in large balloons with diameters ranging from 5 to 8 feet. Though clearly "confined," such balloons were a departure from the highly confined small tube experiments that had been used up to that time, and gave an indication of

combustion properties in "free space." For the 5-ft balloon, detonation of the stoichiometric H_2/air mix required a strong ignition source (2 grams of pentolite explosive). This data revealed that a three-dimensional shock wave could be propagated in "free space" in a H_2/air mix if a sufficiently strong initiator were used. Importantly, ignition of these confined H_2/air stoichiometric mixtures via weak ignition sources (sparks) yielded only fires with no measureable overpressure.

The Little investigators assessed if a larger volume balloon could provide a sufficient path length to allow a transition from fire to deflagration to detonation. Using an 8-foot diameter balloon containing a stoichiometric mixture of hydrogen and air, ignition by weak spark sources produced again only fire with negligible overpressure. The conclusion from this work is that both confinement and explosive initiation are required for the direct explosion of confined hydrogen/air mixtures in which explosion occurs instantaneously. Furthermore, in free space (with no obstacles present), over a distance of ~ 4 feet (the balloon radius), there is no transition of the combustion from fire to deflagration to detonation using weak ignition sources.

In the LH_2 spill tests using 32 gallons in which a vapor cloud forms in the open (no confinement of any kind), the Little researchers found no detonation or tendency towards detonation even when strong explosive initiators were used to ignite the vapor cloud. Since detonation using explosive charges was observed in the 5-foot balloon tests, they concluded that the vapor clouds above real spills had non-ideal mixing that inhibits direct detonation. These observations led the authors to conclude [7], "even with shock-wave initiation, detonation is unlikely of the hydrogen-air cloud from a large-scale spill."

Summarizing these early tests of practical hydrogen combustion risks, direct detonation requires strong ignition sources, confinement, and hydrogen/air mixes within the LEL - UEL range. Weak ignition sources produce fires even when the hydrogen/air mix is within the explosive range and confined in a balloon. Ignition of vapor clouds above sizeable LH_2 releases using strong or weak ignition sources produces only fires. Experimental results for ordinary combustion and detonation were consistent with the LFL – UFL and LEL –UEL ranges listed in Table II. For LNG, ignition tests over LNG pools conducted at Sandia National Laboratories as part of the "Phoenix Program" [38] gave similar results. Ignition of LNG vapors above pools with weak ignition sources produced fires, not deflagrations or explosions.

These experimental results from the 1960s already help frame the hydrogen fire safety issues for the SF-BREEZE. On the Top Deck where the LH_2 is stored, fire is the only credible combustion risk, (rather than detonation, explosion or deflagration) because of the lack of confinement on the top deck and the absence of strong ignition sources. In the confined Starboard and Port Fuel Cell Rooms, direct detonation is not possible because of the lack of strong (intentional) ignition sources. However, we need to examine these fuel cell rooms more carefully to assess the role of confinement and internal obstacles on the acceleration of ordinary fires to deflagrations, with possible subsequent deflagration to detonation transition (DDT).

In the decades since the 1960s, there has been enormous growth in the scientific understanding of hydrogen and methane flammability, deflagration and detonation, which supports and helps understand the A.D. Little test results. This foundational understanding is essential for the design of hydrogen technology systems [37]. Matsui and Lee quantitatively determined [39] the minimum ignition energy required for direct detonation of hydrogen/air and methane/air mixtures and how this threshold energy varies with the fuel/air mix. The minimum ignition energy occurs near the stoichiometric mix (29.53 % for H_2, 9.48 % for methane), and is 4.16 x 10^6 J for hydrogen and 2.28 x 10^8 J for methane. The value for methane is orders of magnitude larger than any other hydrocarbon, making methane exceptionally insensitive to direct detonation. The minimum detonation energy for both hydrogen and methane are ~ 10^8 times larger than the energy required to start normal burning-- an enormous ignition energy requirement essentially precluding direct detonation of hydrogen or methane in accident scenarios.

So far, we have considered three physical limitations to the direct detonation of hydrogen or methane, namely the fuel/air mixture has to be within the range LEL – UEL, a strong (shock wave) initiator is required and the fuel/air mix must be confined. A fourth physical requirement has been discovered over the past several decades: the combustion volume must be larger than the "detonation cell size" of the explosive mixture. As discussed previously by Ng and Lee [37] and Yang [40], it has been experimentally observed that detonations form distinctive physical patterns called "detonation cells" which can be observed in experiments as a "smoke foil" record [41]. For a detonation to occur, the spatial extent of the reacting system must be larger than one cell dimension. For a stoichiometric mix (equivalence ratio = 1) for hydrogen, at room temperature and atmospheric pressure, the detonation cell size is ~ 1.5 cm [41]. The detonation cell size for methane at room temperature and atmospheric press is ~ 33 cm [41]. For the SF-BREEZE Top Deck, and the Starboard and Port Fuel Cell Rooms, the physical dimensions are significantly larger than these detonation cell sizes, meeting the geometry requirement imposed by the detonation cell size. The detonation cell size determines how wide experimental tube reactors must be in the transverse direction (normal to the flame propagation) in order to study tube-based detonations in these gases. If the tube diameter is ~ 13 times the detonation cell size, then a confined planar detonation can transform into an unconfined spherical detonation wave upon exit from the tube [41]. The larger detonation cell size for methane requires using significantly larger tubes or tunnels for experiments than required for hydrogen, making it technically more challenging to examine detonation phenomena in methane.

Deflagration to Detonation Transition (DDT):

Although the absence of strong (intentional) ignition sources precludes the direct detonation of hydrogen and methane in accident scenarios, under certain circumstances it is possible to have a detonation with weak ignition sources given a fuel/air mix within the LEL – UEL range, confinement and obstacles or internal structures within the reacting volume. Unlike direct

detonation, which requires a strong ignition source, this type of explosion can start with a normal fire. In the confined/obstructed environment, the speed of the combustion accelerates over time and distance to a deflagration due to turbulent mixing of the unburnt fuel-air mixture near the obstacles. With further acceleration, the deflagration transitions to a detonation, producing a Deflagration to Detonation Transition (DDT). For H_2, DDT can only occur for 12% fuel /air mix or higher. Both H_2 and NG can experience DDT, although it is easier for hydrogen. Note that for the A.D. Little balloon tests, which showed no acceleration of combustion for either the 5-foot balloon or the 8-foot balloon, there were no internal structures or obstacles which would have promoted a DDT.

The SF-BREEZE Starboard and Port Fuel Cell Rooms (Figure 3) each measure 7.4 m long x 5.1 m wide x 2.7 m tall. These rooms each hold twenty 120 kW fuel cell racks each, which constitute obstacles and potential weak ignition sources for the present discussion. If there were to be a significant hydrogen leak into one of these fuel cell rooms that was not detected by the hydrogen monitors (triggering shutoff of the H_2 supply), or could not be handled by the ventilation system, then the hydrogen buildup, presence of confinement, obstacles and ignition sources could potentially lead to a fire that evolved into a DDT.

An early and particularly illuminating series of DDT tests for H_2/air mixtures was performed at Sandia in the early-mid 1980s in the "FLAME Facility " [42]. Figure 4 gives a diagram of the FLAME facility:

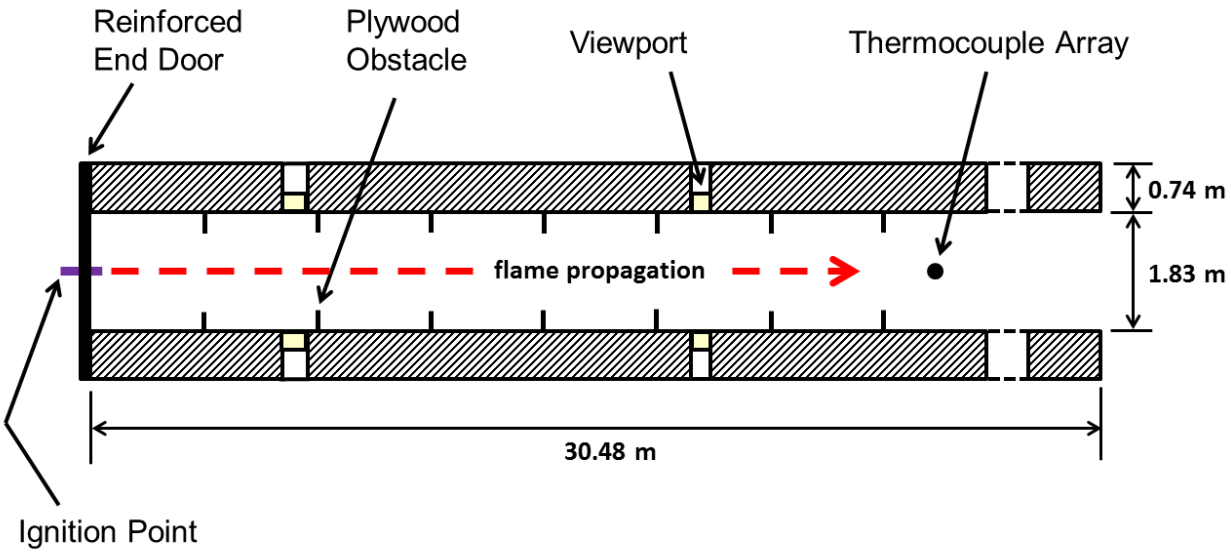

Figure 4: Schematic of the Sandia FLAME facility. Figure is reproduced with modification from Reference 42.

The FLAME tunnel was 1.83 m wide, 2.44 m tall and 30.48 m long, and constructed of heavily reinforced concrete. The transverse dimensions are similar to the 5.1 m x 2.7 m transverse dimensions of the SF-BREEZE Starboard and Port Fuel Cell Rooms. Sherman et al. placed flow obstacles in the tunnel, blocking one third of the cross section of the tunnel (33% blockage ratio), and monitored the speed of combustion as it traversed the FLAME tunnel using thermocouples. The experiments were conducted at atmospheric pressure and ambient temperature.

Figure 5 shows results for the planar flame speed as a function of distance downrange from the ignition end for various H_2/air mixtures in the tunnel with obstacles removed [42].

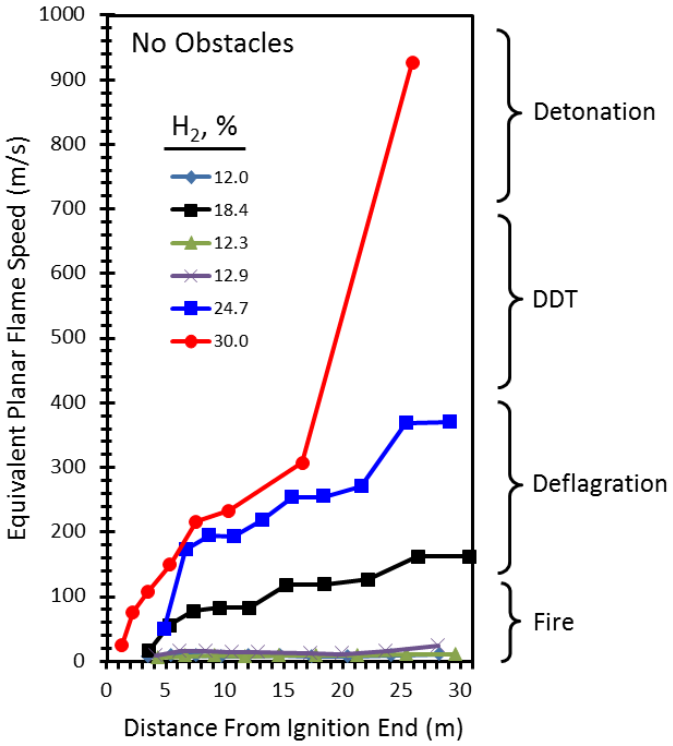

Figure 5: Planar flame speed plotted against distance from the ignition end in FLAME experiments. Obstacles were removed from the tunnel for these measurements. The figure uses data reported in Reference 42.

This figure shows that for hydrogen concentrations of 12.9% or less, the flame velocities are slow, less than ~ 20 m/s. There is no change in the flame velocity as the flame propagates down the tunnel, and thus no flame acceleration occurs with run distance. This is the propagation of an ordinary fire.

However, given confinement, significant downrange run distance and an increase in the hydrogen concentration to 18.4%, one can see in Figure 5 that the flame velocity increases with distance from the ignition end, reaching 162 m/s at the end of the tunnel. Increasing the hydrogen concentration to 24.7%, the flame accelerates to 367 m/s at 25 meters. Qualitatively, we refer to flame speeds in the range ~100 – 400 m/s as "deflagrations" in comparison to the slower "fire" flame speeds at ~ 100 m/s or less. For the 30% mix, a near-stoichiometric mix of hydrogen and air, one sees significant acceleration to 307 m/s at a run distance of 16.6 meters. Thereafter a dramatic jump in flame speed occurs, and the velocity measured 26 meters down the tunnel is a supersonic 927 m/s. This represents the transition from deflagration to detonation. We qualitatively refer to flame speeds from ~ 400 – 700 m/s as being in the "DDT" range, and velocities higher than ~700 m/s as a "detonation." Figure 5 shows how confinement, increasing hydrogen concentration and run distance can cause acceleration from normal fire to deflagration to detonation in relatively confined spaces even if obstacles are absent.

Figure 6 shows the same experiment, only with obstacles placed in the flame propagation path.

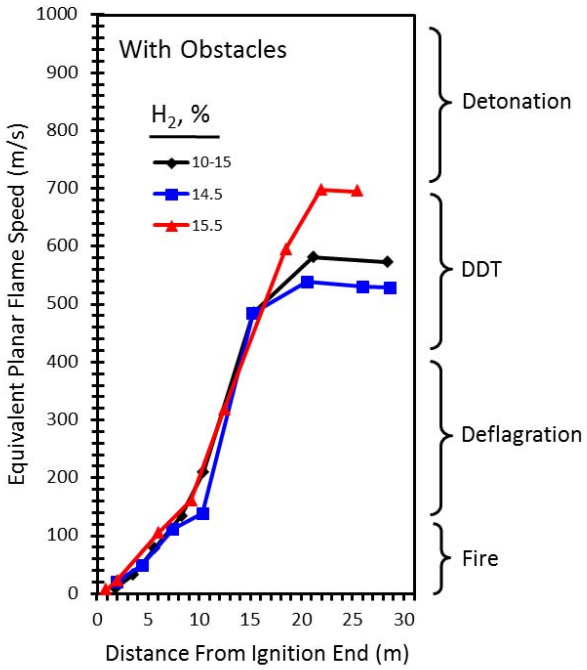

Figure 6: Planar flame speed plotted against distance from the ignition end in FLAME experiments. Obstacles were placed in the tunnel for these measurements. The figure uses data reported in Reference 42. The experiment corresponding to 10 – 15 % hydrogen was one in which a mixing fan lost power, producing an inhomogeneous mixture in which the lower part of the tunnel had 10% hydrogen and the upper part had 15% hydrogen. See Reference 42 for further details.

The presence of obstacles induces an acceleration of the flame velocity at H_2/air concentrations that would otherwise not experience flame acceleration. Given obstacles and a run-up distance of 10 meters, the flame speeds for concentrations greater than 12% accelerate from normal fire speeds to deflagration speeds. With more run time and distance, even at mixtures as low as 15.5%, very fast deflagration velocities of ~ 700 m/s are observed if obstacles are present, corresponding to DDT. The lowest H_2/air mix for which DDT was observed in the Sandia tests was 15% when obstacles where present. Note that the experiment corresponding to 10 – 15 % hydrogen was one in which a mixing fan lost power, producing an inhomogeneous mixture in which the lower part of the tunnel had 10% hydrogen and the upper part had 15% hydrogen [42]. Other studies [43] of large-scale hydrogen/air mixtures have found a lower concentration threshold for hydrogen DDT to be ~ 12.5% in the presence of obstacles.

Recent studies using sophisticated experimental and theoretical approaches have revealed the basic mechanism for DDT [37, 44, 45, 46, 47]. Flame acceleration requires a feedback mechanism between the advancing (initially low-speed laminar) flame and the unburnt fuel/air mix ahead of the flame. Consider the tunnel geometry of the FLAME apparatus in Figure 4. At any given position and moment in time, the flame influences the temperature and pressure in the unburnt flow field ahead of the flame (towards the right in Figure 4). This interaction produces small turbulent structure in the unburnt flow field. When the flame advances and engulfs this turbulence, the flame will burn hotter because the turbulence increases the area of the boundary between flame and unburnt fuel/air (i.e. the flame area increases), and the combustion itself becomes hotter because the fuel and air are better mixed. This increased flame area and temperature affects the new unburnt flow field ahead even more than before, which in turn further increases the combustion energy when, at a later time and downrange distance, the flame encounters this new turbulent area. This feedback continues, increasing the flame speed until the flow reaches the sonic limit consistent with the composition of the combustion products. When the flame speed approaches the speed of sound, shock waves form and shock-flame interactions become an important mechanism for flame wrinkling and further turbulence generation. The deflagration transitions to a detonation at this point.

The role of obstacles is to increase the rate of formation of turbulent structures. For example, obstacles can induce vortices in the upstream flow field, reminiscent of the turbulent structures issuing from aircraft wingtips. As flow moves past the edge of an obstacle, the shear layer can roll up into a spiraling turbulent structure that provides the feedback to the flame needed for an accelerated flame velocity as the flame moves down the tunnel.

Recently, Johansen and Ciccarelli [45] have captured the creation of a turbulent flow field ahead of the advancing flame for stoichiometric methane-air mixtures using a high-speed schlieren video system. The images show directly how the advancing flame affects the unburnt flow field ahead of the flame, the creation of turbulence at obstacles, and how this turbulence alters the

combustion within the flame once the flame passes through the turbulent region. Such experiments have also been successfully modeled theoretically [46].

Figures 5 and 6 showed the importance of "run up distance" in the DDT phenomena. For the Sandia FLAME experiments, 10 meters of run-up distance is needed to attain deflagration speeds of 100 – 200 m/s. In the SF-BREEZE design, the Starboard and Port Fuel Cell Rooms have dimensions 5.1m wide x 2.7 m tall x 7.4 m long. Distributing the PEM fuel cells amongst these two rooms not only creates redundancy in the vessel power system (as required by U.S. Coast Guard regulations), but also limits the run-up distance available to a hydrogen fire should one break out in one of these rooms.

The studies of Groethe and coworkers [48] demonstrate the importance of limited "run-up" in limiting the acceleration of hydrogen combustion caused by obstacles. Their experimental setup is shown in Figure 7:

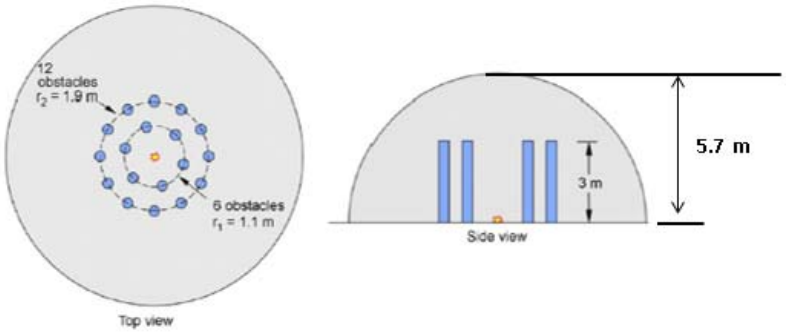

Figure 7: Experimental setup for the experiments reported in Reference 48. Figure reproduced from Reference 48.

A hemispherical tent of radius 5.7 meters (300 m^3 total volume) was outfitted with a weak ignition source (40 J spark) at the hemisphere center, along with 18 cylindrical aluminum cylinders measuring 0.46 m diameter by 3 m height. The cylinders were arranged around a central point of ignition as shown in the Figure 7. Experiments on hydrogen combustion were conducted with and without the cylinders present to assess the role of obstacles in producing DDT in this geometry.

Figure 8 shows optical video images of the combustion using a 30% hydrogen-air volumetric mix [48].

Figure 8: High-speed optical video images of hydrogen combustion for a 30% hydrogen/air mixture, ignited with a 40 J spark. Figure reproduced from Reference 48.

These images show the flame velocity with obstacles present was ~ 85 m/s, consistent with a fast laminar flame. The form of the flame looks like an ordinary fire. Pressure sensors outside the hemispherical tent showed no overpressure produced by the fire of Figure 8 with or without the obstacles placed inside. A reasonable explanation for the lack of obstacle-induced acceleration is that the geometry of Figure 7 does not provide sufficient run-up distance. With only 5.7 m of run-up available, there is insufficient distance for obstacle-induced flame acceleration to occur.

Although the tent provided confinement and an optimal near stoichiometric 30% H_2/air mix, there was no detonation or explosion. This is because a weak ignition source was used. In one experiment, the researchers replaced the weak ignition source with 10 g of C-4 high explosive to initiate the combustion. With a strong ignition source, confinement, the H_2/air mix in the LEL – UEL range, and a geometry larger than the detonation cell size, all the necessary ingredients were in place for a detonation. Figure 9 shows high-speed video images of the detonation.

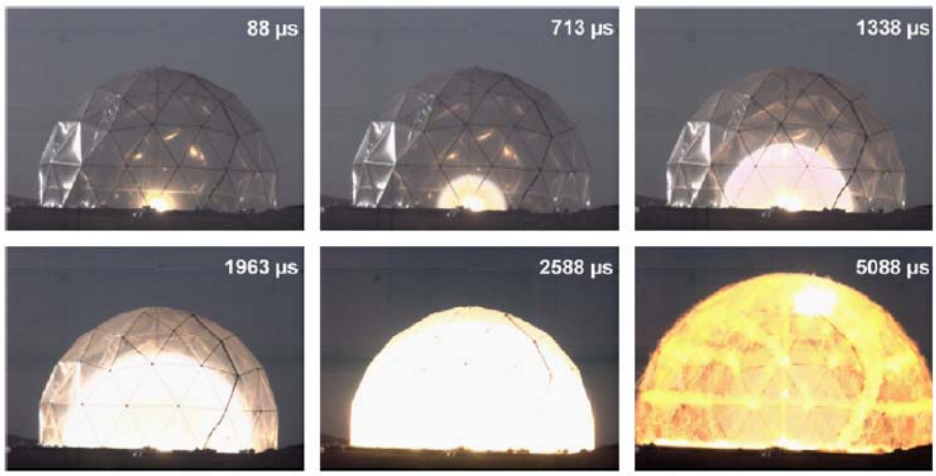

Figure 9: High-speed optical video images of hydrogen combustion for a 30% hydrogen/air mixture, ignited with 10 grams of C-4 high explosive. Figure reproduced from Reference 48.

The time scales in Figure 9 are much shorter than for Figure 8. The video images show that the flame velocity is 1980 m/s, well into the detonation range. Also, note the completely spherical shape of the detonation wave. In a detonation, the flame front advances so rapidly that the fuel/air mixture has essentially no time to move in response to the combustion event. Over the 5088 microseconds of the detonation event, the gas is essentially motionless, with no turbulent structures developed. A nearly perfectly spherical combustion front is created. In contrast, using a weak initiator in Figure 8, over the 65-millisecond duration of the photography the gas volume has time to react to the combustion, producing irregular flame structures. The work of Goethe provides a very educational and intuitive picture of the difference between ordinary combustion and a detonation, in addition to revealing how short run distances can limit DDT even when obstacles are present.

As noted by Sherman et al. [42], from a safety perspective, it not that important if a highly accelerated flame has actually undergone DDT because the overpressures accompanying these phenomena can be similar, producing the same safety hazard. Indeed, we have described the physical phenomena of fire, deflagration, DDT and detonation (explosion) to provide the scientific basis for how hydrogen and natural gas may behave in an accident scenario. All of these combustion phenomena can be dangerous, especially on an isolated vessel, and need to be prevented.

Pool Fires:

One of the striking differences between hydrogen and natural gas is the radiant nature of their fires. When hydrogen burns, the product of combustion is primarily water vapor, with other species such as OH and H radicals, and HO_2 and H_2O_2 produced in trace (< 1 %) amounts. As a result, the vast majority of thermal radiation from hydrogen fires originates from vibrationally excited water molecules. In contrast, when methane burns, although some water is produced, most of the thermal radiation comes from carbon-containing species, and especially carbon soot, which is an efficient radiator of thermal energy. As a result, the thermal radiation emitted from methane fires is (on a fuel LHV basis) 2 - 3 times higher than for a hydrogen fire. This property is quantified as the "radiant fraction," which gives the fraction of fuel combustion energy that is released as radiation. We estimate that for a pool fire involving combustion of the entire 1200 kg of the LH_2 fuel complement, the radiant fraction would be 0.045. A pool fire burning an energy equivalent amount of methane (3198.9 kg) would have a radiant fraction of 0.10. Thus, the methane fire would release 2.2 times more radiant energy than a hydrogen fire for the same combustion energy.

Because a hydrogen fire is emitting infrared (IR) radiation in the vibrational (bending, stretching) modes of water, residual water in the atmosphere is the perfect absorber (and re-emitter) of radiation from hydrogen fires. Thus, humidity in normal air significantly reduces the transmission

of thermal radiation issuing from hydrogen fires. Gerritsma and Haanstra [49] made quantitative measurements of the IR transmission of atmospheric air at room temperature and a relative humidity of 62%. Over a 4.7-meter path length, the average transmission for the water IR bands through the air is 68.2%. Thus, 31.8% of the thermal radiation issuing from a hydrogen fire over a 4.7 m distance would be blocked by atmospheric water vapor [49]. The atmospheric absorption of thermal radiation from a methane fire would be significantly less.

This difference in radiant energy has consequences for the impact fire has on surrounding structures and personnel. In their 1982 study [10], A.D. Little calculated the closest approach one could get to a pool fire of LH_2 and LCH_4 and still not suffer a thermal skin injury (whose threshold was assumed to be 5 kW/m^2) for varying quantities of fuel burned. For a fuel heat content of 144 GJ, corresponding to 1200 kg of LH_2 and 3198.9 kg of LCH_4, calculations were made of the closest approach to the fire in the horizontal direction at grade. For 1200 kg of burning hydrogen, the closest approach is ~ 19 m. For LCH_4, the closest approach is ~ 58 m. One can get closer to a hydrogen fire because it radiates less thermal energy and water vapor in the atmosphere efficiently absorbs and redistributes the IR radiation from a hydrogen fire. These two effects more than compensate for the slightly higher flame temperature of hydrogen compared to methane (Table II).

To bring together the concepts that have been discussed thus far for fuel buoyancy, pool formation, fuel combustion, and fire radiation, it is useful to compare and contrast two hypothetical accident scenarios where the entire 1200 kg LH_2 fuel complement of the SF-BREEZE and the energy equivalent in LNG is instantaneously spilled and ignited on the Top Deck of the vessel. This is a pool fire scenario, which has been the subject of many studies given its importance in fuel and fire safety [50-55]. It was of initial interest to the SF-BREEZE project, because aluminum was used as the material for the Top Deck (to reduce weight), but aluminum is not a structurally strong as steel in traditional (diesel) fires, which initially raised some concerns. Indeed, as specified by Alcan [56], "if a load-bearing structure made from age hardened aluminum alloys is exposed to temperature above 150 °C for several hours, then the residual mechanical characteristics of components made from alloys belonging to the 6000 series will have to be tested after fire." It turns out that the U.S. Coast Guard does <u>not</u> consider the spilling and ignition of the entire fuel complement to be a credible accident scenario for the SF-BREEZE, because there is no history of LH_2 tanks catastrophically failing in this way. Nonetheless, considering this scenario pulls together the hydrogen and methane physical and combustion properties discussed thus far into a worked example.

The energy produced by burning 1200 kg of H_2 is 143,952 MJ, using a LHV value of 119.96 MJ/kg for hydrogen. In the 1982 A.D. Little study [10] of crash scenarios for LH_2 aircraft, predictions were made for pool diameters, duration and flame heights for such a an accident. According to the Little study, 4.5% of the hydrogen combustion energy is converted to thermal radiation (radiant fraction = 0.045). Thus, the thermal energy radiated from burning the 1200 kg of hydrogen from the SF-BREEZE would be 6477.8 MJ. The Little modeling work predicts that spilling 1200 kg (16.90 m^3) of LH_2 would result in a pool of diameter 15 m, yielding a pool fire of

duration 7.2 seconds, and a flame height of 105 m. Given these dimensions for the fire column, and the 6477.8 MJ of radiant energy, the emissive power of the hydrogen fire would be 169.8 kW/m^2 averaged over the entire flame surface during the fire duration of 7.2 seconds. These estimates for the pool diameter and duration for an LH_2 pool fire are consistent with estimates inferred from the cryogen spill investigations and modeling of Verfondern and Dienhart [22]. The result of the instantaneous spill and ignition is to produce a very tall fire. Tall fires do exist, as shown in Figure 10 for a 10-m diameter LNG (consisting of 99% methane) pool fire from the recent Sandia Phoenix tests [54].

Figure 10: A 10-m diameter LNG pool fire from the Sandia Phoenix Tests. Figure reproduced from Reference 54.

The average concentration of hydrogen within the 105 m tall and 15 m diameter combustion column would be 41.9%, well within the LFL – UFL range for hydrogen. The radiant fraction estimated by Little for hydrogen is in reasonable accord with the expectations (13 msec) for the flame residence time calculated for a hydrogen fire column of the dimensions given.

The combustion column is so tall because hydrogen gas is so buoyant. As a result, most of the thermal radiation emitted from the flame surface is directed well above and away from the vessel, with only a small fraction directed downward towards the deck. The percentage of the entire flame area at the base of the fire column is 3.3%. Therefore, thermal radiation directed from the fire to the deck is 213.7 MJ. None of this IR radiation is absorbed directly by the LH_2 pool, because hydrogen is inactive in the IR. The lack of IR absorption by LH_2 pools is an important consideration for quantitative models of LH_2 pool fires. The 213.7 MJ of IR radiation directed downwards passes through the LH_2 pool and strikes the aluminum deck that can absorb the IR radiation. Assuming a conservative (more highly absorbing) emissivity value of 0.4 for aluminum [57], the total thermal energy absorbed by the aluminum Top Deck is 85.5 MJ.

When LH_2 spills (instantaneously in this example) onto the Top Deck of the SF-BREEZE, the hydrogen cools the aluminum deck via the enthalpy of vaporization of the liquid. For a conservative estimate (one that leads to the lowest cooling, and therefore the highest final temperature for the aluminum) we assume a liquid initially at 29 K under pressure, for which the enthalpy of vaporization is 323.9 kJ/kg. Thus, 388 MJ is needed to fully evaporate the 1200 kg of LH_2 fuel. With the dimensions of the Top Deck being 0.794 cm thick, with an area of 162.5 m^2, there is sufficient thermal energy contained in the structure to evaporate all the LH_2. Using the temperature-dependent heat capacity of aluminum, we estimate the final aluminum deck temperature induced by spilling the cryogenic LH_2 fluid would be 168 K.

With 85.5 MJ of radiant energy available to warm up the deck, combined with the energy required to evaporate the LH_2 (which initially cooled the deck) we calculate the final temperature to be 199 K after the sequential LH_2 spill and fire. Thus, through spilling and igniting the LH_2 fuel load on the SF-BREEZE, the final temperature of the deck is below room temperature. There is no structural risk to the aluminum deck, since the temperature during the spill/fire never approaches 150 °C. There is no risk of brittle fracture, since the aluminum Top Deck is not susceptible to brittle fracture [19].

One can perform a similar analysis using an energy equivalent amount of LCH_4, namely 3198.90 kg of LCH_4. Assuming a fuel LHV of 45 kJ/kg to be representative of LNG, the energy produced by burning 3198.9 of methane is 143,952 MJ (same as for burning 1200 kg of hydrogen). Methane fires emit more thermal radiation, since the fuel is based on carbon. We adopt a radiant fraction of 0.10 for methane combustion. Thus, the thermal energy radiated from burning the 3198.9 kg of methane would be 14,395.2 MJ. Scaling results from the analyses of Verfondern and Dienhart [22] we estimate this quantity of LNG would occupy a diameter of 14.0 m and the pool would last 12.3 seconds on the deck. If the fire column height were 87 m (shorter than for H_2 because methane is less buoyant), then the flame surface, for this duration, would have an emissive power of 286 kW/m^2, which is what has been measured in the Phoenix LNG pool fire tests [54].

Note that the average concentration of methane within a column that was 87 m tall and 14 m in diameter would be 25%, outside the UFL range for methane. However, there is little doubt the combination of ignition and density fluctuations within the vapor above the pool would lead to full column combustion. The radiant fraction of 0.10 estimated for methane is in accord with the expectations (34 milliseconds) for the flame residence time calculated for a methane fire column of the dimensions given.

The percentage of the entire methane flame area at the base of the column is 3.7%. Therefore, thermal radiation directed from the fire to the deck is 533 MJ. This value is higher than for hydrogen because of the higher radiant fraction for methane combustion. Unlike the case for hydrogen, LCH_4 is capable of absorbing IR radiation because CH_4 vibrations do involve the creation of a dipole moment. We will ignore this for the present, and assume that all the IR is

directed onto the aluminum deck. Assuming an emissivity of 0.4 for the IR emissivity of aluminum, the total thermal energy absorbed by the aluminum deck is 213 MJ.

When LNG spills (instantaneously in this example) on the Top Deck of the SF-BREEZE, the liquid methane cools the aluminum deck via the enthalpy of vaporization of the liquid. Using the ΔH_{vap} value for LCH_4 of 531 kJ/kg, to evaporate 3198.90 kg of LCH_4 requires 1698 MJ of thermal energy from the SF-BREEZE aluminum deck. This is much larger than the 388 MJ needed to vaporize the LH_2, because the stronger intermolecular forces for methane lead to its higher enthalpy of vaporization. Because the ΔH_{vap} of LCH_4 is so much larger than that for LH_2, the aluminum deck will be cooled down to 111 K, the boiling temperature of LNG, and there will still be LNG left over.

With 213 MJ of radiant energy available from the methane fire to warm up the deck, combined with the energy required to evaporate the LNG (which initially cooled the deck) we can calculate the final temperature to be 198 K, again below room temperature. This is actually quite similar to that calculated for LH_2 (199 K). As was the case with LH_2, there is no structural risk to the Al deck, since the temperature during the spill/fire never approaches 150 °C. There is no risk of brittle fracture, since aluminum does not suffer this materials failure mode [19].

The LH_2 and LNG spill/ignition scenarios produce very similar final temperatures (199 K for LH_2, 198 K for LNG). This is because the 1200 kg of LH_2 cools the 0.794-cm thick aluminum deck less (via its lower ΔH_{vap}) and heats the deck less (via its lower radiant fraction) than the case for spilling and burning 3198.9 kg of LNG. Liquid methane cools the deck significantly more (via its larger ΔH_{vap}), but also warms the deck significantly more (via its larger radiant fraction), with the two effects balancing to produce a similar final aluminum deck temperature as for LH_2.

The Hindenburg:

When considering hydrogen for a new application, for example as a propulsion fuel in the high-speed ferry SF-BREEZE, the existing community often references the Hindenburg accident in 1937. Most people have seen the newsreel images from the accident that tragically claimed the lives of 35 people. In discussions with the maritime community, a common misconception is that the Hindenburg exploded. With the hydrogen combustion properties now sufficiently described, one can look again at the Hindenburg accident with an eye toward the combustion phenomena involved.

It is clear from the photographic record of the event that the accident consisted of a fire, not an explosion. Unlike explosions that are extremely fast (see Figure 9), the airship initially stayed aloft while burning. This is consistent with a fire. The burning airship descended tail-first, because there was still unburned hydrogen in the nose of the airship, due to the relatively slow flame velocity. This also is consistent with a fire. Since the airship provided confinement of the hydrogen, we can conclude that a weak ignition source initiated the hydrogen combustion, not a strong ignition source that would have produced a detonation. Furthermore, there is no evidence

for a DDT from the film record of the event. The lack of explosion and the presence of an ordinary fire do not make the accident any less tragic. Fires are dangerous too, and all effort needs to be directed to preventing hydrogen-based fires. Vessel designs that prevent fires also work to prevent other more dangerous events such as DDT or direct detonation.

In discussions with the maritime community, it has been helpful to provide context for the Hindenburg accident. The Hindenburg held ~15 times more H_2 than the SF-BREEZE. The method of storing hydrogen for the airship (rubberized gas bags) bears no resemblance to the engineered and rugged DOT-approved stainless steel LH_2 tanks in use on the roads today and used in the SF-BREEZE design. Over the past 60 years, NASA has mastered the use of hydrogen, the "signature fuel" of the American Space Program [58]. The Space Shuttle held 102,900 kg of LH_2, 86 times more than the SF-BREEZE [59]. Although there have been two tragic accidents involving the Space Shuttles Challenger and Columbia, these accidents did not originate from the onboard storage or use of LH_2.

Through science-based safety engineering and a sound understanding of hydrogen physical and combustion phenomena, hydrogen technology can be used safely in maritime applications. The 50-year record of transporting LNG throughout the world is excellent: 8 accidents involving spills, with no fires and no fatalities [60]. Since LH_2 and LNG are very similar in their physical and combustion properties, minor augmentation of the proven and effective international regulations for LNG transport will enable regulated and safe use of hydrogen fuel cell technology in maritime applications such as the SF-BREEZE high-speed fuel-cell ferry.

Summary:

The safety-related physical and combustion properties of LH_2 and LNG have been reviewed in the context of the SF-BREEZE high-speed fuel-cell ferry. Due to weaker interaction between molecules, LH_2 is colder than LNG, and evaporates more easily. If spilled, LH_2 cools surfaces less than LNG due to its smaller enthalpy of vaporization, ΔH_{vap}. LH_2 spills are smaller and shorter-lived compared to energy-equivalent LNG spills. LH_2 pool dispersal times for the full 1200 kg of LH_2 spilled on the SF-Breeze deck would be about 6 sec, with a cryogenic pool radius of about 8 m. Permeability is not a leak issue for hydrogen or LNG piping. Hydrogen embrittlement is surmounted by using 304 and 316 stainless steel components for hydrogen rated hardware. Hydrogen embrittlement does not exist for LNG because methane does not dissociate on the Fe-based surfaces (e.g. stainless steel) of pipelines and conventional storage tanks.

LH_2 and LNG are similar in their combustion properties, with hydrogen having a wider flammability range. Vapors of both are easily ignited by weak (thermal) ignition sources and become flammable at low percent volume mixtures with air. H_2 and NG vapors can both directly explode, but require confinement with a geometry larger than the detonation cell size, a strong

(shock wave) initiation source and a fuel/air mixture in the LEL – UEL range for direct detonation. Both fuels can experience DDT depending on the geometry with hydrogen being more susceptible to DDT than methane due in part to its smaller detonation cell size. DDT would be unlikely in the SF-BREEZE application (even in the event of a ventilation failure) because of the lack of confinement on the Top Deck, and the reduced physical dimensions in the Starboard and Port Fuel Cell Rooms that limit "run-up." LH_2 fires burn out faster than LNG fires, and produce significantly less thermal radiation, with the hydrogen fire thermal radiation also strongly absorbed by humidity in the air. In a hypothetical scenario (judged not to be a credible accident threat by the U.S. Coast Guard) where the entire 1200 kg fuel complement of the SF-BREEZE were released and ignited, the temperature of the Top Deck would still be below room temperature due to the combined effects of cryogenic cooling and hydrogen fire radiant heating. Although a LNG spill would cool the aluminum deck more, the higher radiant flux would heat the deck more, producing a similar final temperature. The results show it is safe to use aluminum for the Top Deck of the SF-BREEZE from the point of view of large fuel pool fires because the Top Deck does not approach 150 °C if the fuel complement were spilled and ignited.

Since LH_2 and LNG are similar in their physical and combustion properties, they pose similar safety risks. For both LH_2 and LNG ships, precautions are needed to avoid fuel leaks, minimize ignition sources, minimize confined spaces, provide ample ventilation for confined spaces, and monitor the enclosed spaces to ensure any fuel accumulations are detected and controlled (via H_2 supply shutoff) far below the fuel/air mix thresholds for any type of combustion.

Acknowledgements:

The authors thank Samantha Lawrence and Paul Gibbs (both at Sandia), as well as Jay Keller (Zero Carbon Energy Solutions), Kyle McKeown (Linde), Dave Farese and Brian O'Neil (Air Products), Jim Mullen (Gardner Cryogenics), Karl Verfondern (Research Center Julich) and James Fesmire (NASA) for very helpful discussions. The U.S. Department of Transportation, Maritime Administration (MARAD) funded the SF-BREEZE project. The authors gratefully acknowledge Sujit Ghosh (MARAD) for skillfully managing the project. The work was performed at Sandia National Laboratories, which is a multi-program laboratory managed and operated by Sandia Corporation, a wholly owned subsidiary of Lockheed Martin Corporation, for the U.S. Department of Energy's National Nuclear Security Administration under contract DE-AC04-94AL85000.d

References:

[1]. J. Keller, L. Klebanoff, S. Schoenung and M. Gillie, "The Need for Hydrogen-based Energy Technologies in the 21st Century, Chapter 1 in *Hydrogen Storage Technology, Materials and Applications,* Ed. L.E. Klebanoff (Boca Raton: Taylor & Francis; 2012), p. 3.

[2]. L. Klebanoff, J. Keller, M. Fronk and P. Scott, "Hydrogen Conversion Technologies and Automotive Applications," Chapter 2 in *Hydrogen Storage Technology, Materials and Applications,* Ed. L.E. Klebanoff (Boca Raton: Taylor & Francis; 2012), p. 31.

[3]. J.W. Pratt, L.E. Klebanoff, T. Escher, J. Burgard, C. Leffers and K. Sonerholm, "*Design of the SF-BREEZE High-Speed Fuel-Cell Ferry,*" in preparation.

[4]. J. Hord, "*Is Hydrogen a Safe Fuel?*," Int. J. Hydrogen Energy **3**, 157-176 (1978).

[5]. T.D. Donakowski, "*Is Liquid Hydrogen Safer Than Liquid Methane?*," Fire Technology **17**, 183-188 (1981).

[6]. G.D. Brewer, "*An Assessment of the Safety of Hydrogen-Fueled Aircraft*," J. Aircraft **20**, 935-939 (1983).

[7]. G.D. Brewer, "*Hydrogen Aircraft Technology*," (CRC Press, Boca Raton, 1991).

[8]. A.D. Little, Inc., "*Final Report On An Investigation of Hazards Associated with the Storage and Handling of Liquid Hydrogen*," Report to the U.S. Air Force, C-61092, (1960).

[9]. L.H. Cassutt, F.E. Maddocks, W.A. Sawyer, "*A Study of the Hazards in Storage and Handling of Liquid Hydrogen,*" Report to the U.S. Air Force, Report No. 61-05-5182, (1964).

[10]. A.D. Little, Inc., "*An Assessment of the Crash Fire Hazard of Liquid Hydrogen Fueled Aircraft,*" Final Report to the National Aeronautics and Space Administration, NASA CR-165526 (1982).

[11]. A. Contreras, S. Yigit, K.Ozay and T.N. Veziroglu, "*Hydrogen as Aviation Fuel: A Comparison with Hydrocarbon Fuels,*" Int. J. Hydrogen Energy **22**, 1053-1060 (1997).

[12]. G.A. Karim, "*Some Considerations of the Safety of Methane, (CNG), as an Automotive Fuel- Comparison with Gasoline, Propane and Hydrogen Operation,*" SAE Technical Paper Series 830267 (1983).

[13]. See for example: M. Hajbabaei, G. Karavalakis, K.C. Johnson, L. Lee and T.D. Durbin, "*Impact of Natural Gas Fuel Composition on Criteria, Toxic and Particle Emissions from*

Transit Buses Equipped with Lean Burn and Stoichiometric Engines," Energy **62**, 425-434 (2013).

[14]. J.D. Naber, D.L. Siebers, S.S. DiJulio and C.K. Westbrook, "*Effects of Natural Gas Composition on Ignition Delay Under Diesel Conditions,*" Combustion and Flame **99**, 192-200 (1994).

[15]. S. Bates and D.S. Morrison, "*Modelling the Behavior of Stratified Liquid Natural Gas in Storage Tanks: A Study of the Rollover Phenomenon,*" Int. J. Heat Mass Transfer **40**, 1875-1884 (1997).

[16]. The densities of cold hydrogen and methane gases are taken from the NIST database: http://webbook.nist.gov/cgi/fluid.cgi?T=160+K&PLow=0.99+atm&PHigh=1.03+atm&PInc=.1&Applet=on&Digits=5&ID=C74828&Action=Load&Type=IsoTherm&TUnit=K&PUnit=atm&DUnit=kg%2Fm3&HUnit=kJ%2Fmol&WUnit=m%2Fs&VisUnit=uPa*s&STUnit=N%2Fm&RefState=DEF).

[17]. B. Bowman and L. Klebanoff, "*Historical Perspectives on Hydrogen, Its Storage, and Its Applications,*" Chapter 3 in *Hydrogen Storage Technology, Materials and Applications,* Ed. L.E. Klebanoff (Boca Raton: Taylor & Francis; 2012), p. 65.

[18]. R.E. Reed-Hill and R. Abbaschian, "*Physical Metallurgy Principles*," (PWS Publishing, Boston, 1994), p.740.

[19]. M.G. Zabetakis, "*Safety with Cryogenic Fluids,*" (Plenum, New York, 1967), p. 25.

[20]. R.D. Witcofski and J.E. Chirivella, "*Experimental and Analytical Analyses of the Mechanisms Governing the Dispersion of Flammable Clouds Formed by Liquid Hydrogen Spills,*" Int. J. Hydrogen Energy **9**, 425-435 (1984).

[21]. K. Verfondern and B. Dienhart, "*Experimental and Theoretical Investigations of Liquid Hydrogen Pool Spreading and Vaporization,*" Int. J. Hydrogen Energy **22**, 649-660 (1997).

[22]. K. Verfondern and B. Dienhart, "*Pool Spreading and Vaporization of Liquid Hydrogen*," Int. J. Hydrogen Energy **32**, 2106 – 2117 (2007).

[23]. P. Middha, M. Ichard and B. J. Arntzen, "*Validation of CFD Modelling of LH_2 Spread and Evaporation Against Large-scale Spill Experiments,*" Int. J. Hydrogen Energy **36**, 2620-2627 (2011).

[24]. C. San Marchi, B.P. Somerday and S.L. Robinson, "*Permeability, Solubility and Diffusivity of Hydrogen Isotopes in Stainless Steels at High Gas Pressures,*" Int. J. Hydrogen Energy **32**, 100-116 (2007).

[25]. G. Wedler and M. Mengel, "*The Adsorption of Methane on Polycrystalline Iron Films,*" Surface Science **131**, L423-L428 (1983).

[26]. D.C. Sorescu, "*First-principles Calculations of the Adsorption and Hydrogenation Reactions of CH_x (x = 0, 4) Species on a Fe(100) Surface,*" Phys. Rev. B **73**, 155420 (2006).

[27]. A. Staykov, J. Yamabe and B.P. Somerday, "*Effect of Hydrogen Gas Impurities on the Hydrogen Dissociation on Iron Surface,*" Int. J. Quantum Chemistry **114**, 626-635 (2014).

[28]. F. Bozso, G. Ertl, M. Grunze and M. Weiss, "*Chemisorption of Hydrogen on Iron Surfaces,*" Appl Surf. Sci. **1**, 103-119 (1977).

[29]. The hydrogen embrittlement of metals is extensively reviewed in the books: "*Gaseous Hydrogen Embrittlement of Materials in Energy Technologies,*" Vol. 1 and 2, ed. R.P. Gangloff and B.P. Somerday (Woodhead Publishing Ltd., Cambridge, 2012).

[30]. Kyle McKeown (Linde), private communication to L.E. Klebanoff on November 2, 2015.

[31]. Some of the gaseous hydrogen properties listed are from: L.M. Das, "*Hydrogen Engines: A View of the Past and a Look Into the Future,*" Int. J. Hydrogen Energy **15**, 425-443 (1990).

[32]. F.L. Dryer, M. Chaos, Z. Zhao, J.N. Stein, J.Y. Alpert and C.J. Homer, "*Spontaneous Ignition of Pressurized Releases of Hydrogen and Natural Gas into Air,*" Combust. Sci. and Tech. **179**, 663-694 (2007).

[33]. G.R. Astbury and S.J. Hawksworth, "*Spontaneous Ignition of Hydrogen Leaks: A Review of Postulated Mechanisms,*" Int. J. Hydrogen Energy **32**, 2178-2185 (2007).

[34]. T. Mogi, Y. Wada, Y. Ogata and A. K. Hayashi, "*Self-ignition and Flame Propagation of High-pressure Hydrogen Jet During Sudden Discharge from a Pipe,*" Int. J. Hydrogen Energy **34**, 5810-5816 (2009).

[35]. K.L. Cashdollar, I.A. Zlochower, G.M. Green, R.A. Thomas and M. Hertzberg, "*Flammability of Methane, Propane and Hydrogen Gases,*" J. Loss Prevention in the Process Industries **13**, 327-340 (2000).

[36]. R.W.Schefer, G.H. Evans, J. Zhang, A.J. Ruggles and R. Greif, "*Ignitability Limits for Combustion of Unintended Hydrogen Releases: Experimental and Theoretical Results,*" Int. J. Hydrogen Energy **36**, 2426-2435 (2011).

[37]. H.D. Ng and J.H.S. Lee, "*Comments on Explosion Problems for Hydrogen Safety," J. Loss Prevention in the Process Industries,*" **21**, 136-146 (2008).

[38]. A. Luketa and T. Blanchat, "*The Phoenix Series Large Scale Methane Gas Burner Experiments and Liquid Methane Pool Fire Experiments on Water*," Combustion and Flame **162**, 4497-4513 (2015).

[39]. H. Matsui and J.H. Lee, "*On the Measure of the Relative Detonation Hazards of Gaseous Fuel-Oxygen and Air Mixtures,*" Symposium (International) on Combustion **17**, 1269-1280 (1979).

[40]. J.M. Yang, "*An Improved Analytical Approach to Determine the Explosive Effects of Flammable Gas-Air Mixtures,"* Report UCRL-TR-217005 Lawrence Livermore National Laboratory, November 2005 (available from osti.gov).

[41]. R. Knystautas, C. Guirao, J.H. Lee and A. Sulmistras, "*Measurements of Cell Size in Hydrocarbon-Air Mixtures and Predictions of Critical Tube Diameter, Critical Initiation Energy and Detonability Limits,*" Progress in Astronautics and Aeronautics, Volume **94**, American Institute of Aeronautics and Astronautics (AIAA), 1984.

[42]. M.P. Sherman, S.R. Tieszen and W.B. Benedick, "*FLAME Facility: The Effect of Obstacles and Transverse Venting on Flame Acceleration and Transition to Detonation for Hydrogen-Air Mixtures at Large Scale,*" Sandia National Laboratories Report SAND85-1264 R3, 1989.

[43]. S.B. Dorofeev, V.P. Sidorov, A.E. Dvoinishnikov and W. Breitung, "*Deflagration to Detonation Transition in Large Confined Volume of Lean Hydrogen-Air Mixtures,*" Combustion and Flame **104**, 95-110 (1996).

[44]. E.S. Oran and V.N. Gamezo, "*Origins of the Deflagration-to-Detonation Transition in Gas-phase Combustion,*" Combustion and Flame **148**, 4 – 47 (2007).

[45]. C.T. Johansen and G. Ciccarelli, "*Visualization of Unburned Gas Flow Field Ahead of An Accelerating Flame in an Obstructed Square Channel,*" Combustion and Flame **156**, 405-416 (2009).

[46]. D.A. Kessler, V.N. Gamezo and E.S. Oran, "*Simulations of Flame Acceleration and Deflagration-to-Detonation Transitions in Methane-Air Systems,*" Combustion and Flame **157**, 2063-2077 (2010).

[47]. P. Middha and O.R. Hansen, "*Predicting Deflagration to Detonation Transition in Hydrogen Explosions,*" Process Safety Progress **27**, 192 -204 (2008).

[48]. M. Groethe, E. Merilo, J. Colton, S. Chiba, Y. Sato and H. Iwabuchi, "*Large-scale Hydrogen Deflagrations and Detonations,*" Int. J. Hydrogen Energy **32**, 2125-2133 (2007).

[49]. C.J. Gerritsma and J.H. Haanstra, "*Infrared Transmission of Air Under Laboratory Conditions,*" Infrared Physics **10**, 79-90 (1970).

[50]. V. Babrauskas, "*Estimating Large Pool Fire Burning Rates,*" Fire Technology **19**, 251 – 261 (1983).

[51]. D.W. Hissong, "*Keys to Modeling LNG Spills on Water,*" J. Hazardous Materials **140**, 465-477 (2007).

[52]. A. Luketa-Hanlin, "*A Review of Large-scale LNG Spills: Experiments and Modeling,*" J. Hazardous Materials **A132**, 119-140 (2006).

[53]. J.A. Fay, "*Model of Large Pool Fires,*" J. Hazardous Materials **B136**, 219-232 (2006).

[54]. A. Luketa, "*Recommendations on the Prediction of Thermal Hazard Distances from Large Liquefied Natural Gas Pool Fires on Water for Solid Flame Models,*" Sandia National Laboratories Report SAND2011-9415, (2011).

[55]. P.K. Raj, "*Large Hydrocarbon Pool Fires: Physical Characteristics and Thermal Emission Variations with Height,*" J. Hazardous Materials **140**, 280-292 (2007).

[56]. A summary of the fire properties of Aluminum has been written by Alcan Marine, and can be found at:
http://www.ansatt.hig.no/henningj/materialteknologi/Lettvektdesign/Al%20and%20the%20sea/Alcan+anglais+chap.09.pdf

[57]. C.-D. Wen and I. Mudawar, " *Emissivity Characteristics of Roughened Aluminum Alloy Surfaces and Assessment of Multispectral Radiation Thermometry (MRT) Emissivity Models,*" Int. J. of Heat and Mass Transfer **47**, 3591-3605 (2004).

[58]. A description of LH_2 becoming the signature fuel for NASA can be found at:
http://www.nasa.gov/topics/technology/hydrogen/hydrogen_fuel_of_choice.html

[59]. James Fesmire (NASA), private communication to J.W. Pratt on April 22, 2016.

[60]. M. Hightower, L. Gritzo, A. Luketa-Hanlin, J. Covan, S. Tieszen, G. Wellman, M. Irwin, M. Kaneshige, B. Melof, C. Morrow and D. Ragland, "*Guidance on Risk Analysis and Safety Implications of a Large Liquefied Natural Gas (LNG) Sill Over Water,*" Sandia National Laboratories Report: SAND2004-6258, December (2004).